Deep-level transient spectroscopy of $TiO_2/CuInS_2$ heterojunctions

Marian Nanu,[a] Florence Boulch, Joop Schoonman, and Albert Goossens
Laboratory for Inorganic Chemistry, Delft Institute for Sustainable Energy, Delft University of Technology, Julianalaan 136, 2628 BL Delft, The Netherlands

(Received 26 September 2005; accepted 2 November 2005; published online 7 December 2005)

Deep-level transient spectroscopy (DLTS) has been used to measure the concentration and energy position of deep electronic states in $CuInS_2$. Flat $TiO_2|CuInS_2$ heterojunctions as well as TiO_2-$CuInS_2$ nanocomposites have been investigated. Subband-gap electronic states in $CuInS_2$ films are mostly due to antisite point defects and vacancies. Substitution of indium with copper, Cu^{II}_{In}, leads to an acceptor state 0.15 eV above the valence band, while copper vacancies, V^{I}_{Cu}, are acceptor states at 0.1 eV. Furthermore, indium on a copper position, In''_{Cu}, yields a donor state at 0.07 eV below the conduction band, while sulphur vacancies are donor states at 0.0=eV. With DLTS, these states are indeed found. For flat configurations, V^{I}_{Cu} are the dominant acceptors with a concentration of 1.83×10^{17} cm^{-3}. In contrast for nanocomposites Cu^{II}_{In} are the dominant acceptors having a concentration of 6.7×10^{17} cm^{-3}. We conclude that the concentration of antisite defects in nanocomposite $CuInS_2$ is significantly higher than that in flat films of $CuInS_2$. © *2005 American Institute of Physics*. [DOI: 10.1063/1.2140611]

In recent years, solar cell technology—based on the ternary compound semiconductors, such as $CuInSe_2$, $CuGaSe_2$,$CuInS_2$, and their multinary alloys Cu(In,Ga)$\times$(Se,S)$_2$—have been advanced.[1–4] Within this family, $CuInS_2$ is considered a promising candidate because of its high absorption coefficient and its direct band gap of E_g =1.5 eV, which is well matched to the solar spectrum.[5] Native defects, introduce energy levels in the band gap of CIS which leads to recombination.[6] Indeed, a correlation between the density of a deep bulk states and the open-circuit voltage of $CuInS_2$ solar cells has been found.[7]

Deep-level transient spectroscopy (DLTS) is used to determine the energy position and the concentration of deep electronic states.[8] In DLTS, the occupancy of a trap is perturbed by applying a forward bias pulse. After removing the bias, a high-energy situation is created and depopulation of the filled deep levels sets in. By performing capacitance measurements as function of time, this depopulation process can be monitored. Repeating the measurements at different temperatures provides the activation energy for the depopulation process.

Since Lang[9] introduced DLTS in 1974, this technique has been applied extensively to characterize deep levels in semiconductors. In the present investigations, a novel approach to DLTS is used to determine the energy position and concentrations of deep electronic states in $CuInS_2$. In our DLTS experiments, the junction capacitance is measured at different frequencies. High frequencies are used to measure the donor-type defects, while at low frequencies the junction capacitance is dominated by the acceptor type defects, which are deeper in energy.

Flat $TiO_2|CuInS_2$ heterojunctions and TiO_2–$CuInS_2$ nanocomposites have been investigated. For flat heterojunctions, 100 nm dense anatase TiO_2 films are obtained with spray pyrolysis. To form a nanostructured heterojunction on top of the dense anatase TiO_2 film, 2 μm thick nanoporous TiO_2 films are deposited using doctor blading. CIS films are deposited by atomic layer deposition (ALD), as described elsewhere.[10] Finally, electrical contacts of evaporated gold with a diameter of 2 mm are applied.

DLTS has been performed with an EGG 283 potentiostat as the voltage source and a frequency response analyzer (Solartron 1255) coupled to a computer interface. To measure the capacitance, a 10 mV ac voltage is superimposed onto the dc bias voltage. The modulation frequency window spanned six decades, i.e., between 0.5 Hz and 1 MHz.

The explicit form of the time dependence of the capacitance is:

$$C(t) = C_0 + \Delta C \exp[-t/\tau], \tag{1}$$

where τ^{-1} is the emission rate, e_p, of the released charges, C_0 is the capacitance prior to the filling pulse, and ΔC represent the difference between the capacitance at the beginning and at the end of the filling pulse.

The hole emission rate depends on the temperature as follows:

$$e_p = 1/\tau_= \gamma T^2 \sigma_{pa} \exp(-E_{pa}/kT), \tag{2}$$

where σ_{pa} is the capture cross section, γ is a constant equal to $3.25\times10^{21}(m_p/m_0)$, where m_p is the effective hole mass being 1.3 m_0,[11] E_{pa} is the thermal activation energy, k is the Boltzmann constant, and T is the temperature. A plot of $\ln(\tau T)$ versus $(1/T)$ yields a straight line with a slope of (E_{pa}/k), from which the energy of the involved electronic state can be determined. In addition, the y-axis intercept of $\ln(1/\gamma\sigma_{pa})$ yields to the capture cross section.

Furthermore, the trap density N_t can be calculated using the following expression:

$$Nt = N_A x(\Delta C/C_0). \tag{3}$$

The effective acceptor density can be determined from capacitance-voltage measurements.

In the present study, DLTS is performed in a temperature interval from 130 to 400 K. Capacitance transients are mea-

[a]Electronic mail: m.nanu@tnw.tudelft.nl

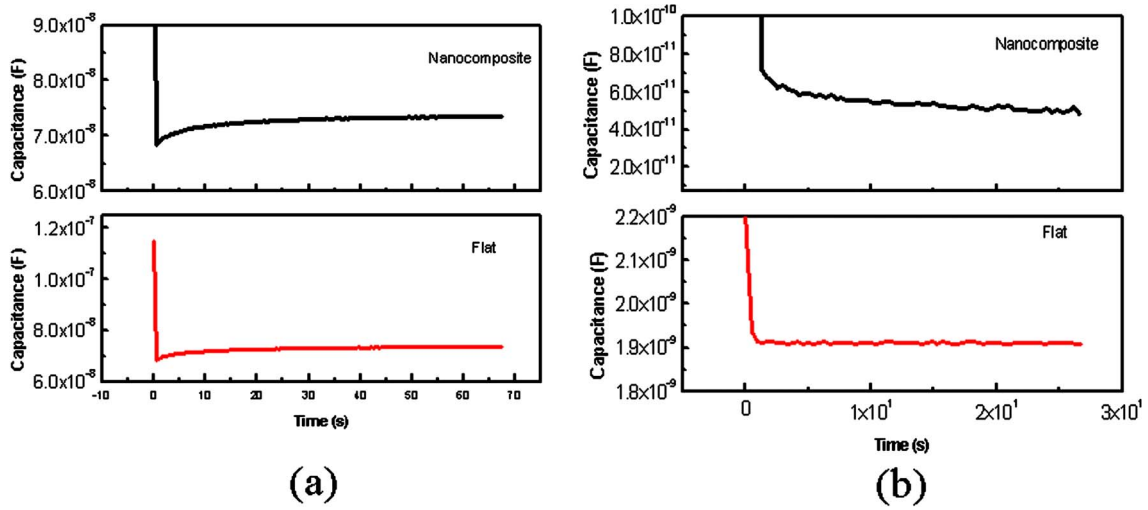

FIG. 1. Representative capacitance transients recorded at a quiescent voltage (*Vb*) of −0.6 V and a pulse height of 0.5 V. The ac modulation, from which the capacitance is derived, is 1 Hz for graph (a) and 1 MHz for graph (b) for flat and nanocomposite heterojunctions.

sured up to 30 s after the filling pulse is applied. The filling pulse duration width is in the range of 0.1–10 s, with a bias voltage limited to approximately −1 V.

Figure 1 shows two representative capacitance transients recorded after a filling pulse of 0.5 V from −0.6 to −0.1 V. Before and after the filling pulse, a constant bias voltage of −0.6 V is maintained. The modulation frequency is varied between 1 Hz [Fig. 1(a)] and 1 MHz [Fig. 1(b)]. Upon applying this filling pulse, both minority and majority carriers are injected in $CuInS_2$ by which the occupation of deep acceptor and donor states are changed. From the temperature dependence of the capacitance transients, we determine the activation energies of the depopulation process. A value of 0.107 eV is found for the majority carriers while 0.04 eV is obtained for the minority carriers (Fig. 2). When these values are compared with photoluminescence studies of $CuInS_2$, the majority carrier activation energy is related to the presence of copper vacancies (V^{I}_{Cu}) while the activation energy for the minority carriers is related to the presence of sulphur vacancies (V''_{S}).[12]

The duration of the filling pulse does not influence the recorded DLTS data; when the pulse time is varied from 0.03 s to 10 s, no changes in the thermal activation energy are found. This suggests that the trap centers can be considered to be isolated points defects and that the energy distribution of the electronic states is small. On the other hand, the modulation frequency does have a significant influence on the DLTS signal. As is shown in Fig. 1, for frequencies higher than 500 kHz the minority carrier-type DLTS signal is recorded, while at frequencies between 0.5 Hz and 10 kHz majority type signals are found. Within these frequency windows, the activation energies that are derived have an insignificant frequency dependency. These results are different then the ones reported by Siemer *et al.*,[13] which may be due to differences in the preparation of $CuInS_2$. In dense $CuInS_2$ deposited by ALD, the predominant defects appear to be related to copper and sulphur vacancies. The presence of a deeper state could not be found, which suggests that for flat films the concentrations of deeper states related to Cu–Au order, i.e., Cu^{II}_{In} and In''_{Cu} have relatively low concentrations.

ALD is a self-limiting method allowing layer-by-layer growth to yield conformal deposition on textured surfaces. One could thus expect that the same quality of the absorber semiconductor can be obtained for flat and three-dimensional (3D) devices. However, although the same deposition parameters have been used for the deposition of $CuInS_2$ inside nanoporous TiO_2 and onto dense TiO_2, different properties are obtained for the two cases. CIS thin films grown with atomic layer-chemical vapor deposition are *p*-type semiconductors, due to the presence of copper ion vacancies V^{I}_{Cu}, indium ion vacancies V^{III}_{In} or antisite acceptor defects Cu^{II}_{In}, which are charge compensated by holes. If deviation from stoichiometry is small, Cu^{II}_{In} antisite defects are accompanied by a donor antisite defect In''_{Cu}. The presence of these antisite

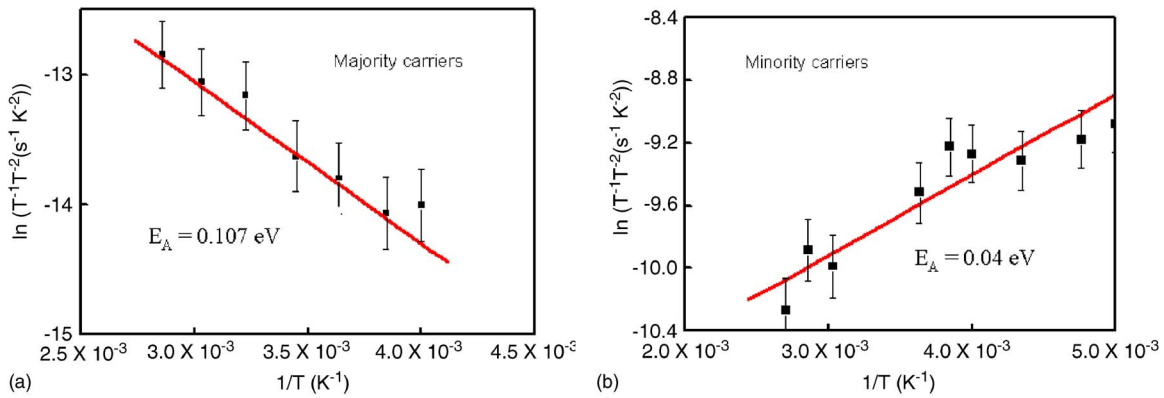

FIG. 2. Activation energy of minority (a) and majority (b) charge traps in the subband gap of $CuInS_2$ that form flat heterojunctions.

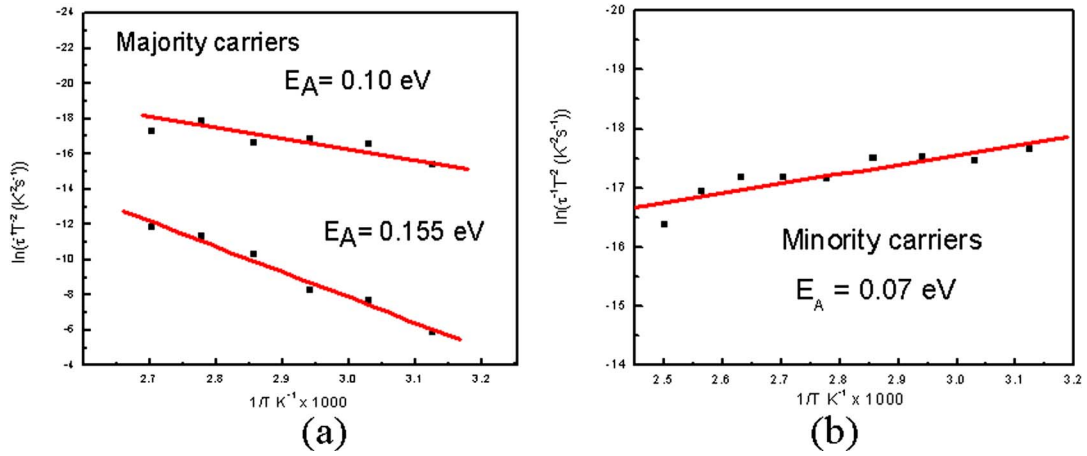

FIG. 3. Activation energy of minority (a) and majority (b) charge traps in the subband gap of $CuInS_2$ that form nanocomposite heterojunctions.

TABLE I. Capture cross section of the minority and majority carriers determined by DLTS.

Sample morphology	Type of defects	Activation energy (eV)	Capture cross section (cm^2)	Density of traps (cm^{-3})
Flat	Majority V_{Cu}^{I}	0. 107	3.9×10^{-17}	5×10^{13}
Flat	Minority V_{S}''	0.04	4.4×10^{-18}	1.8×10^{13}
Nanostructured	Majority Cu_{In}^{II} or V_{In}^{III}	0.155	8×10^{-15}	2×10^{14}
Nanostructured	Majority V_{Cu}^{I}	0.1	7.2×10^{-17}	1×10^{13}
Nanostructured	Minority In_{Cu}''	0.07	3.2×10^{-17}	1×10^{14}

defects is related to the occurrence of Cu–Au ordering. The degree of the Cu–Au ordering is larger for $CuInS_2$ deposited into the nanostructured TiO_2 matrix than when $CuInS_2$ is deposited on dense substrates, as has been discussed in previous studies.[14,15]

Similar to the flat film configuration, the majority type signal in nanocomposites is recorded at low modulation frequencies, while the minority type is recorded at high modulation frequencies [Figs. 1(a) and 1(b)]. The thermal activation energy of electron traps in the nanocomposite $CuInS_2$ is found to be 0.07 eV [Fig. 3(b)], while the activation energies for hole traps are 0.1 eV and 0.155 eV [Fig. 3(a)]. When these results are compared to those for thin films where two new defects are found, i.e., a predominant level for electron trapping at 0.07 eV, assigned to In_{Cu}'', and a new activation energies for hole trap at 0.155 eV assigned to Cu_{In}^{II}. These defects, which are related to the Cu–Au order, have the highest concentration and dominate the trapping process. These results support our previous conclusions and confirm that Cu–Au ordering is higher in a nanocomposite configuration compared to that in flat films. Like in flat films, as well as for 3D films, no influence of the filling duration on the emission rate has been observed.

Capture cross section of the minority and majority carriers are determined from the intercept of the Arrhenius plots using Eq. (2). The results are given in Table I.

To calculate the trap concentration, the net acceptor concentration (N_A-N_D) of the semiconductor, that forms the *p-n* heterojunctions, is measured using capacitance-voltage measurements. An effective N_A-N_D concentration of 2×10^{18} cm^{-3} is found.

With DLTS, the influence of the geometry, i.e., flat films or nanocomposites on the electrical properties of the *p*-type $CuInS_2$, has been investigated. ALD-deposited $CuInS_2$ on the dense TiO_2 exhibits one electron-trap and one hole-trap center, at 0.04 eV and 0.1 eV, respectively. If $CuInS_2$ is deposited in a nanostructured matrix, the deep acceptor and donor concentrations become larger. The characteristic activation energy states related to the presence of Cu–Au disorder is observed in this case, i.e., a donor state localized at 0.07 eV and an acceptor state at 0.155 eV. Moreover, it is found that the activation energies do not depend on the duration of the filling pulse. These results are in line with our previous studies, but differ from other DLTS studies on $CuInS_2$.

[1]J. A. M. AbuShama, S. Johnston, T. Moriarty, G. Teeter, K. Ramanathan, and R. Noufi, Prog. Photovoltaics **12**, 39 (2004).
[2]M. Rusu, S. Doka, C. A. Kaufmann, N. Grigorieva, T. Schedel-Niedrig, and M. C. Lux-Steiner, Thin Solid Films **480**, 341 (2005).
[3]R. Scheer, T. Walter, H. W. Schrock, M. L. Fearheiley, and H. J. Lewerenz, Appl. Phys. Lett. **63**, 3294 (1993).
[4]K. Ramanathan, M. A. Contreras, C. L. Perkins, S. Asher, F. S. Hasoon, J. Keane, D. Young, M. Romero, W. Metzger, R. Noufi, J. Ward, and A. Duda, Prog. Photovoltaics **11**, 225 (2003).
[5]K. Fukuzaki, S. Kohiki, H. Yoshikawa, S. Fukushima, T. Watanabe, and I. Kojima, Appl. Phys. Lett. **73**, 1385 (1998).
[6]J. Krustok, J. Raudoja, and H. Collan, Thin Solid Films **387**, 195 (2001).
[7]T. Walter, A. Content, K. O. Velthaus, and H. W. Schock, Sol. Energy Mater. Sol. Cells **26**, 357 (1992).
[8]D. K. Schroder, *Semiconductor Material and Device Characterization* (Wiley, New York, 1998).
[9]D. V. Lang, J. Appl. Phys. **45**, 3023 (1974).
[10]M. Nanu, J. Schoonman, and A. Goossens, Chem. Vap. Deposition **10**, 45 (2004).
[11]D. K. Schroder, *Semiconductor Material and Device Characterization*, 2nd ed. (Wiley-Interscience New York, 1998).
[12]M. Nanu, J. Schoonman, and A. Goossens, Thin Solid Films **451**, 193 (2004).
[13]K. Siemer, J. Klaer, I. Luck, and D. Braunig, Thin Solid Films **387**, 222 (2001).
[14]M. Nanu, J. Schoonman, and A. Goossens, Adv. Funct. Mater. **15**, 95 (2005).
[15]M. Nanu, J. Schoonman, and A. Goossens, Adv. Mater. (Weinheim, Ger.) **16**, 453 (2004).